Published in final edited form as:
Nature. 2002 November 14; 420(6912): 193–198. doi:10.1038/nature01201.

The heteromeric cyclic nucleotide-gated channel adopts a 3A:1B stoichiometry

Haining Zhong[*], **Laurie L. Molday**[†], **Robert S. Molday**[†], and **King-Wai Yau**[*,‡,§]

[*]Department of Neuroscience, Johns Hopkins University School of Medicine, Baltimore, Maryland 21205, USA

[‡]Department of Ophthalmology, Johns Hopkins University School of Medicine, Baltimore, Maryland 21205, USA

[§]Howard Hughes Medical Institute, Johns Hopkins University School of Medicine, Baltimore, Maryland 21205, USA

[†]Department of Biochemistry and Molecular Biology, and Department of Ophthalmology, University of British Columbia, Vancouver, British Columbia, Canada V6T 1Z3

Abstract

Cyclic nucleotide-gated (CNG) channels are crucial for visual and olfactory transductions[1–]4. These channels are tetramers and in their native forms are composed of A and B subunits5, with a stoichiometry thought to be 2A:2B (refs 6, 7). Here we report the identification of a leucine-zipper8-homology domain named CLZ (for carboxy-terminal leucine zipper). This domain is present in the distal C terminus of CNG channel A subunits but is absent from B subunits, and mediates an inter-subunit interaction. With cross-linking, non-denaturing gel electrophoresis and analytical centrifugation, this CLZ domain was found to mediate a trimeric interaction. In addition, a mutant cone CNG channel A subunit with its CLZ domain replaced by a generic trimeric leucine zipper produced channels that behaved much like the wild type, but less so if replaced by a dimeric or tetrameric leucine zipper. This A-subunit-only, trimeric interaction suggests that heteromeric CNG channels actually adopt a 3A:1B stoichiometry. Biochemical analysis of the purified bovine rod CNG channel confirmed this conclusion. This revised stoichiometry provides a new foundation for understanding the structure and function of the CNG channel family.

Distinct A subunits (or α-subunits) of vertebrate CNG channels, named CNGA1–4 according to the latest nomenclature5, mediate rod phototransduction (A1), cone phototransduction (A3) and olfactory transduction (A2 and A4). Two B subunits (orβ-subunits) are known, named CNGB1 and CNGB3 (CNGB2 does not exist5), with CNGB1 being part of native rod and olfactory channels and CNGB3 part of cone channels. When expressed heterologously, most A subunits (CNGA1–3) form functional homomeric channels1[–]4; in contrast, B subunits do not, but they form functional heteromers with A subunits. Homologues of these A and B subunits have been identified in *Drosophila*[9] and *Caenorhabditis elegans*[10,11].

While examining possible inter-domain interactions of the human (h)CNGA3 subunit, we found that its cytoplasmic C terminus, designated A3-C, interacted with itself. Thus, when co-

Correspondence and requests for materials should be addressed to R.S.M. (molday@unixg.ubc.ca). or K.-W.Y. (kyau1@jhem.jhmi.edu)..

Competing interests statement The authors declare that they have no competing financial interests.

Note added in proof: After submission of this paper, we found that ref. 31 also proposed a 3A:1B stoichiometry, although no experimental data were provided.

expressed in HEK 293T cells, haemagglutinin (HA)-tagged A3-C could be co-immunoprecipitated with Myc-tagged A3-C by an anti-Myc antibody (Fig. 1a). This homotypic interaction was confirmed by an *in vitro* binding assay in which purified recombinant glutathione S-transferase (GST)-tagged and His-tagged A3-C were found to interact directly with each other (Fig. 1b). Furthermore, when 293T cells transfected with Myc-tagged A3-C were metabolically labelled and lysed, a single radioactive protein species with the expected molecular mass was immunoprecipitated by the anti-Myc antibody (Fig. 1c), confirming that no other proteins mediated the homotypic interaction. Finally, similar homotypic interactions were seen with C-terminal constructs of CNGA1 (bovine) and CNGA2 (rat) (Fig. 1d). The C terminus of CNGB1 (human) showed only very weak interaction (data not shown), and that of CNGB3 (mouse) showed no detectable interaction (Fig. 2b, right gel).

Sequence analysis identified a 22-residue leucine-zipper-like sequence (underlined in Fig. 2a) in the C terminus of hCNGA3, downstream of the cyclic-nucleotide-binding site. Deleting these residues abolished the homotypic interaction of a molecule comprising the last 114 residues of A3-C (Fig. 2b, compare A3C-28/A3C-28 and A3C-32/A3C-32 lanes). Further deletion and truncation analyses (Fig. 2b, see A3C-71/A3C-71; also data not shown) revealed that the full interaction domain covers the 22-amino-acid sequence plus 25 residues immediately downstream. This domain, which we name CLZ, is present in all examined CNG channel A subunits (Fig. 2a) but not in the B subunits. It consists of two leucine-zipper-like coiled-coils connected out of phase by a hydrophilic linker. At least several conserved leucine or hydrophobic residues (marked by asterisks in Fig. 2a) are important: when any of them was mutated into alanine, the homotypic interaction was undetectable in the co-immunoprecipitation assay (data not shown). Finally, the CLZ domain was able to confer homotypic interaction on the C terminus of CNGB3 when inserted after the cyclic nucleotide-binding site (Fig. 2b, right gel).

Despite the importance of the CLZ domain, its disruption only weakened, but did not abolish, the interaction of the complete A3-C, in that the construct A3C-ΔZ (Fig. 2b, see A3C-ΔZ/A3C-ΔZ lane) still showed a mild interaction. Further experiments suggested that a region upstream of the CLZ domain also interacts homotypically, but the CLZ-mediated interaction is much stronger (data not shown). From here on, we shall focus on the CLZ domain.

In a gel-filtration experiment, a C-terminal fragment (A3C-28; see Fig. 2b) of hCNGA3 having the CLZ domain as the only interacting motif was found to be fractionated into a peak with an apparent molecular mass (estimated from its Stoke's radius) 3.5-fold that of the monomer peak (Fig. 3a; see Methods). Because the heterotetrameric CNG channel contains at least one B subunit, which does not contain the CLZ domain, this result suggests that the fragment probably forms a trimer rather than a tetramer. Indeed, a similar experiment with a slightly larger C-terminal fragment of the channel (T565-End) gave a value of 3.1 (data not shown).

Because the gel-filtration result could have been confounded by molecular shape, we did a cross-linking experiment on A3C-28 with dithiobis-succinimidyl propionate (DSP), a cross-linker cleavable by reducing reagents. Partial cross-linking produced three bands in SDS-PAGE under non-reducing conditions, but only one band in the presence of dithiothreitol (Fig. 3b). These bands presumably represented the monomer, dimer and trimer, respectively. More complete cross-linking shifted the product mostly to the highest (trimer) band. This cross-linking was CLZ-dependent because, when this domain was disrupted (A3C-32 in Fig. 3b), only the lowest (monomer) band was observed. Similar results were obtained for the corresponding C-terminal constructs of hCNGA1 and rat CNGA2 (Fig. 3c), confirming generality among A subunits.

To be definitive, a native-gel approach was used. A3C-28 migrated on a native gel primarily as multimers, as supported by the observation that a point mutant (A3C-87: L633A; Fig. 3d, upper gel) with a disrupted homotypic interaction migrated much more rapidly than the wild type. We constructed two other mutants of A3C-28, retaining the homotypic interaction but with extra negative (A3C-88: K596E, R603E) or positive (A3C-89: D613K, E615K) charges. As expected, A3C-88 had a much higher mobility than A3C-89 in native-gel electrophoresis (Fig. 3d, upper gel). When co-expressed, these two mutants gave four bands (Fig. 3d, upper gel), consistent with the combinatorial possibilities, P_3, P_2Q, PQ_2 and Q_3, from two proteins P and Q that form trimers. The four bands became particularly evident when the transfected complementary DNA ratio for A3C-88 and A3C-89 was manipulated (Fig, 3d, lower gel).

The final evidence came from analytical centrifugation, a method of determining the molecular mass independently of shape. A 48-residue peptide (Lys 624–Gly 671) corresponding to the CLZ domain was synthesized and analysed by equilibrium sedimentation. The resulting data were best fitted if the peptide formed a trimer, rather than a dimer or tetramer, in solution (Fig. 3e).

To examine whether the CLZ domain forms a trimer in the context of the complete channel protein, we replaced this domain in hCNGA3 with well-characterized leucine zippers[12] that form dimers, trimers and tetramers, respectively. All mutants readily formed homomeric channels when expressed alone (Fig. 4a). However, the mutants harbouring dimeric and tetrameric leucine zippers consistently differed, although moderately, from the wild-type channel in the $K_{1/2}$ value of the dose-response relation (Fig. 4b) and in the saturated cAMP-activated/saturated cGMP-activated current ratio[13] (Fig. 4c). In contrast, the mutant harbouring a trimeric leucine zipper mimicked the wild type fairly well in both properties. Furthermore, like the wild type, the trimeric mutant gave comparable currents in the absence and presence of the B subunit, but not the dimeric and tetrameric mutants (Fig. 4d). Thus, the CLZ domain was best emulated by a generic trimeric leucine zipper in functional CNG channels.

The fact that the trimeric CLZ domain is present only in the A subunits but not the B subunits seems to leave only one natural stoichiometry, 3A:1B, for the hetero-tetrameric CNG channel. To examine this hypothesis directly, we purified the native CNG channel from bovine rod photoreceptor membranes by affinity chromatography and determined the relative amounts of A and B subunits in the channel complex. The native rod channel consists of a truncated A subunit (CNGA1) and a large B subunit (CNGB1) that migrate on SDS gels as polypeptides of apparent molecular masses 68,000 and 240,000 (M_r 68K and 240K), respectively[14,15] (Fig. 5a). We quantified the relative tryptophan contents in these bands from the fluorescence arising from ultraviolet-induced trichloroethanol-modified residues[16] (Fig. 5b). The ratio of tryptophan signals for the A:B subunits was 1.5 ± 0.4 (mean ± s.d.) (n = 10), in close agreement with the predicted ratio of 1.3 for a 3A:1B stoichiometry but not with the ratio of 0.4 for a 2A:2B stoichiometry (the truncated A subunit has 9 tryptophan residues; the B subunit has 21). We also determined the relative cysteine contents of the A and B subunits labelled by the fluorescent Oregon Green maleimide (Fig. 5c). The observed modified cysteine ratio of 1.8 ± 0.5 (n = 3) for A:B bands was also closer to the predicted ratio of 1.2 for a 3A:1B stoichiometry than the ratio of 0.4 for a 2A:2B stoichiometry (the A subunit has 6 cysteine residues; the B subunit has 15). The higher than expected value observed in our experiments might arise from the limited accessibility of some cysteine residues in the GARP (glutamic-acid-rich protein) part[15] of the B subunit to the bulky Oregon Green maleimide compound. Finally, we examined whether the channel subunits were degraded during purification. Only intact A and B subunits were detected on western blots labelled with a variety of monoclonal antibodies against different epitopes on these subunits (see Fig. 5d for an example). The absence of degraded fragments indicates that no significant proteolysis of the channel had occurred. Together, our data support a stoichiometry of 3A:1B for the native rod CNG channel.

Our results refute the current belief that the CNG channel adopts a 2A:2B composition, which was largely supported by two studies on the rod channel[6,7]. One study[6] relied on a Ni^{2+} potentiation of the opening of homomeric bovine (b)CNGA1 channels by coordinating corresponding histidine residues (His 420) of two adjacent subunits[17]; the corresponding residue in bCNGB1 is asparagine (Asn 546). These authors found that Ni^{2+} potentiated the heteromeric channel whether formed by wild-type bCNGA1 and bCNGB1 or by reciprocally mutated bCNGA1 (H420Q) and bCNGB1 (N546H), concluding that there was an AABB stoichiometry/ordering. However, their implicit assumption was that Ni^{2+} acted only on the histidine residue in question, whereas others[7] have reported that a mild potentiation by Ni^{2+} persisted in the heteromeric channel formed by wild-type bCNGB1 and mutant bCNGA1 (H420Q). The second study[7] arrived at an ABAB stoichiometry/ordering based on expressions and co-expressions of the tandem dimers A–A, A–B, B–A and B–B. This conclusion assumed that only the leading subunit, not the trailing subunit, of a tandem dimer could incorporate singly into a functional channel. Otherwise, the data would be consistent with a 3A:1B stoichiometry.

In summary, our results suggest that the preferred stoichiometry of heteromeric CNG channels is 3A:1B, although it is impossible to rule out a small percentage of native CNG channels with a different stoichiometry. The olfactory CNG channel is composed of two A subunit species (CNGA2 and CNGA4) and one B subunit species (CNGB1b)5,18–21. Because these A subunits both contain the CLZ domain, the native channel is expected to contain one B subunit together with two A2 and one A4, or one A2 and two A4, subunits (previous work on the stoichiometry of channels formed by co-expressed A2 and A4 is unfortunately not informative because the B subunit was absent22). Our findings also provide perhaps the first example of a breakdown of symmetry in tetrameric channels. Previous studies based on homomeric CNG channels have suggested that the four CNG subunits in a channel complex are organized into two functional dimers23,24. A three-dimensional structure of purified rod CNG channel at 35Å resolution25 also suggests that the intracellular domains are arranged as a pair of dimers. Incorporating these findings, the linker between the cyclic-nucleotide-binding site and the CLZ domain might be flexible enough that, despite its asymmetric composition, the other parts of the CNG channel can still configure and function as a `dimer of dimers'.

Methods

Molecular biology

All of the cDNAs expressed in HEK 293T cells were subcloned into a pRK5 vector. GST fusion proteins were subcloned into pGEX-4T2 (Pharmacia), and His-tagged fusion proteins into pET-28c (Novagene). All mutants were made by standard methods.

Co-immunoprecipitation

The experiments were performed in IP buffer (1 × PBS, 5mM EDTA, 5mM EGTA and 1mMβ-mercaptoethanol). At 2 days after transfection using calcium phosphate, the HEK 293T cells were lysed in 1% Triton X-100 and centrifuged at 100,000*g* for 10 min. The soluble fraction was incubated with a monoclonal anti-Myc antibody (9E10; Roche) and Protein G–Sepharose (Amersham Pharmacia) for more than 2 h. The beads were washed once with 1% Triton, twice with 1% Triton plus 500mM NaCl, and twice with IP buffer. The precipitate was eluted with Laemmli buffer and subjected to western analysis with the anti-Myc antibody and an anti-HA antibody (2013819; Roche).

In vitro binding

GST and His-tag fusion proteins were prepared in accordance with commercial protocols. Three μg of each protein was added to a final volume of 0.5 ml IP buffer plus 1% Triton. After

overnight rocking at 4 °C, glutathione–Sepharose beads (Pharmacia) were added to the reactions and were rocked for 1.5 h. The beads were then washed and eluted similarly to those for the co-immunoprecipitation experiment.

Metabolic labelling

At 2 days after transfection, 293T cells were starved for sulphur for 25 min in a cysteine-free methionine-free medium. A mixture of [^{35}S]cysteine and [^{35}S]methionine (NEG-772; NEN; 1mCi per 60-mm dish) was added to the medium and growth was allowed for 3 h before the cells were lysed and subjected to immunoprecipitation. The precipitate was separated by SDS–PAGE. The gel was dried before autoradiographic exposure.

Gel filtration

Transfected 293T cells were lysed by freezing and thawing twice. The lysate was rocked at 4 °C for 30 min and centrifuged for 11min at 100,000*g*. A fast-protein-liquid-chromatography (FPLC) controller (LCC-500; Pharmacia) was used to fractionate the lysate on a Superdex-200 gel-filtration column (Amersham-Pharmacia) at a flow rate of 0.5 ml min^{-1}. Fractions were collected at half-minute intervals and subjected to western analysis with the anti-HA antibody. The signals on the film were scanned and quantified.

Cross-linking

Transfected 293T cells were lysed as described for gel-filtration experiments. A cross-linking reagent (DSP; Pierce) cleavable by reducing reagents was added to the lysate at different concentrations from a 50-mM stock in dimethyl sulphoxide (DMSO). The reaction was stopped after 30 min by Laemmli buffer with or without reducing reagent (40mM dithiothreitol). The result was analysed by western blotting with the anti-HA antibody.

Native gel

A continuous gel (10% polyacrylamide) was prepared with the Bio-Rad mini-gel setup. The gel and electrode buffers were 0.1M Tris-phosphate titrated to pH 7.3 with Tris base. Protein samples were prepared as in gel-filtration experiments, but with added 10% glycerol and 0.01% bromophenol blue (final concentrations) to facilitate loading. The gel was run at a constant 100V for 7.5 h, then soaked for more than 10min in buffer used for standard SDS–PAGE (0.1% SDS, 25mM Tris and 190mM glycine) to denature the proteins. The gel was subjected to conventional protein transfer and western blotting.

Analytical centrifugation

A peptide was dissolved and dialysed in 1 × PBS, 1mM EDTA, and samples (0.5, 1 or 2mgml^{-1}) were loaded into double-sector centrifugation cells with 12-mm (125-μl) or 3-mm (32-μl) EPON centrepieces and centrifuged at 4 °C at 40,000, 45,000 and 52,000 r.p.m., respectively (Beckman Optima XL-I). Optical absorbance was measured after equilibrium. The data were analysed by global nonlinear least-squares fits with the NONLIN program[26]. M_r and partial specific volume were calculated with Sedenterp version 1.06 (ref. 27).

Electrophysiology

Inside-out excised-patch recordings were made as described[28].

Determination of ratio of A:B subunits

The native rod CNG channel was purified from hypotonically lysed bovine rod outer segments by a calmodulin–Sepharose or PMc 1D1 anti-channel monoclonal-antibody–Sepharose column as previously described[29]. The samples were run on 7% SDS–PAGE for Coomassie

Blue staining and fluorescence detection of modified tryptophan after the ultraviolet-induced reaction of tryptophan with 5% trichloroethanol as described[16]. Relative cysteine contents of the A and B subunits were determined by labelling the purified rod CNG channel with 2mgml^{-1} Oregon Green maleimide (Molecular Probes) for 1 hr at 4 °C in the presence of 1% SDS and 20 μg Tris[2-carboxyethyl]phosphine hydrochloride (Pierce) prior to SDS-gel electrophoresis. Oregon Green maleimide labelling of the channel was completely inhibited by previous treatment with 10mM N-ethylmaleimide. The modified tryptophan fluorescence was quantified with a Fluorchem 8000 Digital Imaging System (Alpha Innotech Corp., San Leandro, CA). The fluorescence from the Oregon Green maleimide-labelled channel subunits was quantified with a Typhoon 8600 variable mode imager. In each case, the fluorescence signal was proportional to the amount of protein applied to the gel. The western blots shown in Fig. 5d were labelled with a mixture of the PMc 1D1 and PMb 3C9 monoclonal antibodies against the A and B subunits as described previously[14,15]. In separate experiments, antibodies against other epitopes were also used but are not shown (PMc 6E7, PMc 2G11, Garp 1H5 and PMs 5E11)[14,15,30].

Acknowledgments

We thank R. Huganir, P. Kim, D. Leahy, M. Li, J. Nathans, F. Rupp and D. Yue for advice and suggestions; members of the Yau laboratory for comments on the manuscript; M. Biel for the mCNGB3 cDNA; P. Kim for providing us with peptide samples corresponding to dimeric, trimeric and tetrameric leucine zippers; and M. Rodgers for helping us in the analytical centrifugation experiment. This work was supported by grants from the US National Eye Institute to K.-W.Y. and R.S.M.

References

1. Finn JT, Grunwald ME, Yau KW. Cyclic nucleotide-gated ion channels: an extended family with diverse functions. Annu. Rev. Physiol 1996;58:395–426. [PubMed: 8815801]
2. Zagotta WN, Siegelbaum SA. Structure and function of cyclic nucleotide-gated channels. Annu. Rev. Neurosci 1996;19:235–263. [PubMed: 8833443]
3. Biel M, Zong X, Ludwig A, Sautter A, Hofmann F. Structure and function of cyclic nucleotide-gated channels. Rev. Physiol. Biochem. Pharmacol 1999;135:151–171. [PubMed: 9932483]
4. Kaupp UB. Family of cyclic nucleotide gated ion channels. Curr. Opin. Neurobiol 1995;5:434–442. [PubMed: 7488843]
5. Bradley J, Frings S, Yau KW, Reed R. Nomenclature for ion channel subunits. Science 2001;294:2095–2096. [PubMed: 11764791]
6. Shammat IM, Gordon SE. Stoichiometry and arrangement of subunits in rod cyclic nucleotide-gated channels. Neuron 1999;23:809–819. [PubMed: 10482246]
7. He Y, Ruiz M, Karpen JW. Constraining the subunit order of rod cyclic nucleotide-gated channels reveals a diagonal arrangement of like subunits. Proc. Natl Acad. Sci. USA 2000;97:895–900. [PubMed: 10639176]
8. Alber T. Structure of the leucine zipper. Curr. Opin. Genet. Dev 1992;2:205–210. [PubMed: 1638114]
9. Baumann A, Frings S, Godde M, Seifert R, Kaupp UB. Primary structure and functional expression of a *Drosophila* cyclic nucleotide-gated channel present in eyes and antennae. EMBO J 1994;13:5040–5050. [PubMed: 7957070]
10. Coburn CM, Bargmann CI. A putative cyclic nucleotide-gated channel is required for sensory development and function in *C. elegans*. Neuron 1996;17:695–706. [PubMed: 8893026]
11. Komatsu H, Mori I, Rhee JS, Akaike N, Ohshima Y. Mutations in a cyclic nucleotide-gated channel lead to abnormal thermosensation and chemosensation in *C. elegans*. Neuron 1996;17:707–718. [PubMed: 8893027]
12. Harbury PB, Zhang T, Kim PS, Alber T. A switch between two-, three-, and four-stranded coiled coils in GCN4 leucine zipper mutants. Science 1993;262:1401–1407. [PubMed: 8248779]

13. Gordon SE, Oakley JC, Varnum MD, Zagotta WN. Altered ligand specificity by protonation in the ligand binding domain of cyclic nucleotide-gated channels. Biochemistry 1996;35:3994–4001. [PubMed: 8672432]
14. Molday RS, et al. The cGMP-gated channel of the rod photoreceptor cell characterization and orientation of the amino terminus. J. Biol. Chem 1991;266:21917–21922. [PubMed: 1718987]
15. Korschen HG, et al. A 240 kDa protein represents the complete beta subunit of the cyclic nucleotide-gated channel from rod photoreceptor. Neuron 1995;15:627–636. [PubMed: 7546742]
16. Kazmin D, Edwards RA, Turner RJ, Larson E, Starkey J. Visualization of proteins in acrylamide gels using ultraviolet illumination. Anal. Biochem 2002;301:91–96. [PubMed: 11811971]
17. Gordon SE, Zagotta WN. Subunit interactions in coordination of Ni^{2+} in cyclic nucleotide-gated channels. Proc. Natl Acad. Sci. USA 1995;92:10222–10226. [PubMed: 7479756]
18. Bradley J, Li J, Davidson N, Lester HA, Zinn K. Heteromeric olfactory cyclic nucleotide-gated channels: a subunit that confers increased sensitivity to cAMP. Proc. Natl Acad. Sci. USA 1994;91:8890–8894. [PubMed: 7522325]
19. Liman ER, Buck LB. A second subunit of the olfactory cyclic nucleotide-gated channel confers high sensitivity to cAMP. Neuron 1994;13:611–621. [PubMed: 7522482]
20. Sautter A, Zong X, Hofmann F, Biel M. An isoform of the rod photoreceptor cyclic nucleotide-gated channel beta subunit expressed in olfactory neurons. Proc. Natl Acad. Sci. USA 1998;95:4696–4701. [PubMed: 9539801]
21. Bonigk W, et al. The native rat olfactory cyclic nucleotide-gated channel is composed of three distinct subunits. J. Neurosci 1999;19:5332–5347. [PubMed: 10377344]
22. Shapiro MS, Zagotta WN. Stoichiometry and arrangement of heteromeric olfactory cyclic nucleotide-gated ion channels. Proc. Natl Acad. Sci. USA 1998;95:14546–14551. [PubMed: 9826737]
23. Root MJ, MacKinnon R. Two identical noninteracting sites in an ion channel revealed by proton transfer. Science 1994;265:1852–1856. [PubMed: 7522344]
24. Liu DT, Tibbs GR, Paoletti P, Siegelbaum SA. Constraining ligand-binding site stoichiometry suggests that a cyclic nucleotide-gated channel is composed of two functional dimers. Neuron 1998;21:235–248. [PubMed: 9697867]
25. Higgins MK, Weitz D, Warne T, Schertler GF, Kaupp UB. Molecular architecture of a retinal cGMP-gated channel: the arrangement of the cytoplasmic domains. EMBO J 2002;21:2087–2094. [PubMed: 11980705]
26. Johnson ML, Correia JJ, Yphantis DA, Halvorson HR. Analysis of data from the analytical ultracentrifuge by nonlinear least-squares techniques. Biophys. J 1981;36:575–588. [PubMed: 7326325]
27. Laue, TM.; Shah, BD.; Ridgeway, TM.; Pelletier, SL. Analytical Ultracentrifugation in Biochemistry and Polymer Science. Harding, SE.; Rowe, AJ.; Horton, JC., editors. Royal Society of Chemistry; Cambridge, UK: 1992. p. 90-125.
28. Chen TY, Yau KW. Direct modulation by Ca^{2+}-calmodulin of cyclic nucleotide-activated channel of rat olfactory receptor neurons. Nature 1994;368:545–548. [PubMed: 7511217]
29. Molday RS, Molday LL. Purification, characterization, and reconstitution of cyclic nucleotide-gated channels. Methods Enzymol 1999;294:246–260. [PubMed: 9916231]
30. Poetsch A, Molday LL, Molday RS. The cGMP-gated channel and related glutamic acid-rich proteins interact with peripherin-2 at the rim region of rod photoreceptor disc membranes. J. Biol. Chem 2001;276:48009–48016. [PubMed: 11641407]
31. Kaupp UB, Seifert R. Cyclic nucleotide-gated ion channels. Physiol. Rev 2002;82:769–824. [PubMed: 12087135]

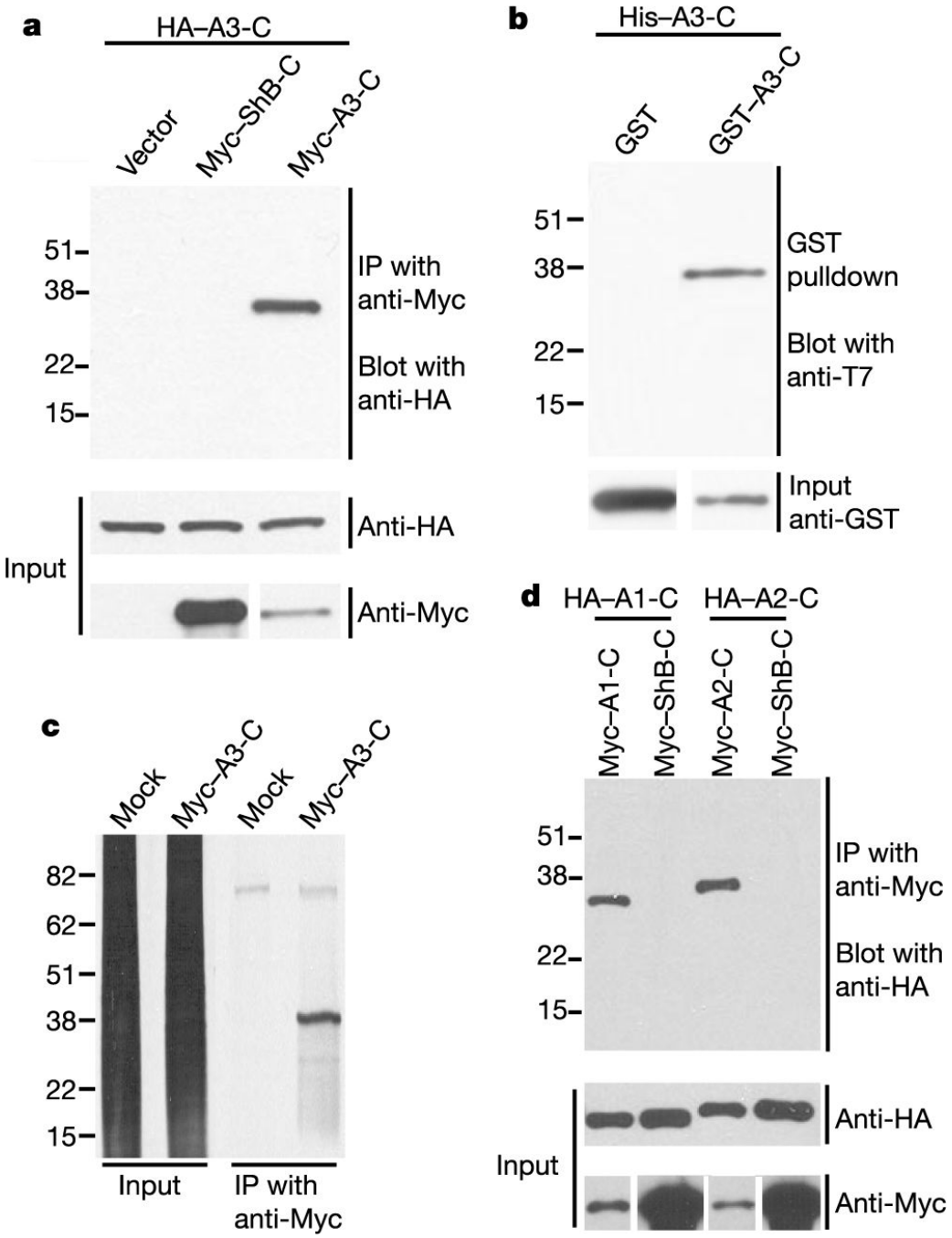

Figure 1.

Homotypic interaction of the C terminus of CNG channel A subunit. **a**, Co-immunoprecipitation of epitope-tagged C termini of CNGA3. The constructs were amino-terminally tagged with HA (MGYPYDVPDYADLNGGGGGST) or Myc (MEQKLISEEDLNGGGGGST). The constructs were: A3-C, start of cytoplasmic C terminus (Asn 398) to end of human CNGA3; ShB-C, Asn 482 to end of Shaker B potassium channel (negative control). Inputs before immunoprecipitation (IP) are shown at the bottom and artificially aligned to save space. **b**, Binding *in vitro*. The His-tagged protein was detected with an antibody (69522; Novagen) against a T7 epitope right after the His tag. The inputs of GST (control) and the GST-tagged protein, detected with an anti-GST antibody (27-4577-01;

Amersham), before binding *in vitro* are also shown and are artificially aligned (bottom). **c**, Metabolic labelling. 293T cells transfected with Myc-tagged A3-C were metabolically labelled, then immunoprecipitated with the anti-Myc antibody. The pulled-down proteins and inputs before the immunoprecipitation are shown (see Methods). **d**, Co-immunoprecipitation of epitope-tagged C-termini of CNGA1 and CNGA2. The experiment was as described in **a**. The constructs were: A1-C, Asn 393 to end of bovine CNGA1; A2-C, Asn 372 to end of rat CNGA2. Numbers alongside the gels are relative molecular mass (M_r) values in kD.

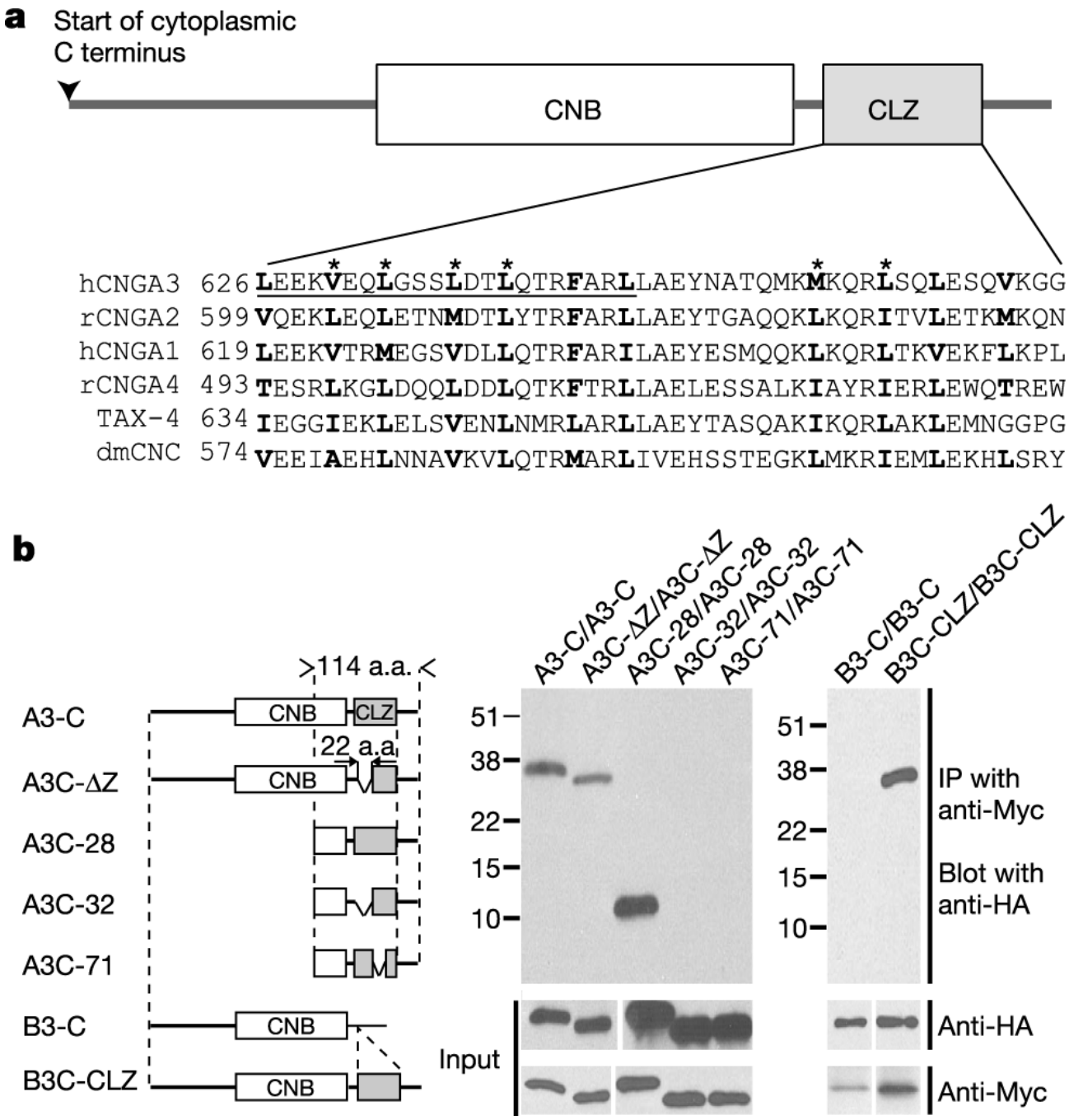

Figure 2.

Identification of the CLZ domain. **a**, Cytoplasmic C terminus of CNG channel A subunit, showing the cyclic-nucleotide-binding domain (CNB) and the CLZ domain. Sequence alignments of the CLZ domains of vertebrate and invertebrate CNG channel A subunits are shown underneath. dmCNC and Tax-4 are those of *Drosophila* and *C. elegans*, respectively. Conserved hydrophobic residues are in bold type. The 22-residue leucine zipper first identified by sequence analysis is underlined. Asterisks label hydrophobic residues found to be essential for the CLZ interaction of hCNGA3 in the co-immunoprecipitation assay. Prefixes: h, human; r, rat. **b**, Homotypic interactions of various C-terminal constructs of hCNGA3 and mouse (m) CNGB3. In all lanes, the indicated front construct is HA-tagged and after construct is Myc-

tagged. The inputs are arbitrarily aligned. The constructs are: A3C-ΔZ, A3-C with Leu 626 to Leu 647 deleted; A3C-28, Lys 581 to end of hCNGA3; A3C-32, A3C-28 with Leu 626 to Leu 647 deleted; A3C-71, A3C-28 with Leu 648 to Arg 661 deleted; B3-C, Gln 432 to end of mCNGB3; B3C-CLZ, B3-C with Ala 655 to Phe 658 replaced by Lys 624 to Gly 672 of hCNGA3 plus two extra residues (Val-Glu) for facilitating insertion by restriction enzymes. a.a., amino acids. Numbers alongside the gels are M_r values in *K*.

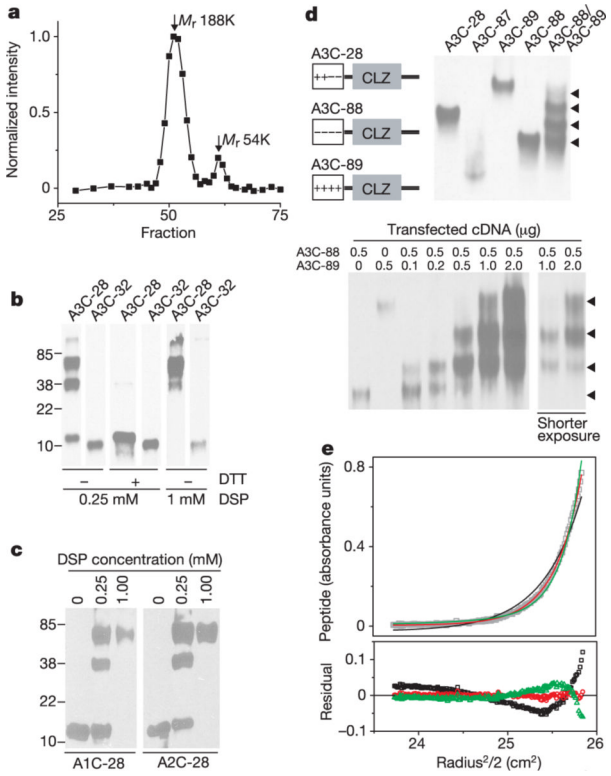

Figure 3.

The CLZ domain forms a trimer. **a**, Gel-filtration experiment with N-terminally HA-tagged A3C-28 (see Fig. 2b). See Methods for details. The M_r values of the peaks were estimated from their Stokes radii based on a standard curve (not shown). **b**, Cross-linking experiment on N-terminally HA-tagged A3C-28 or A3C-32 (CLZ-disrupted A3C-28, see Fig. 2b) with the cross-linker DSP. The faint >100K band in the gels seems to be non-specific. DTT, dithiothreitol. **c**, Cross-linking experiments on HA-tagged A1C-28 (Lys 574 to end of human CNGA1) and A2C-28 (Lys 555 to end of rat CNGA2). **d**, Native-gel electrophoresis. All constructs were N-terminally HA-tagged and detected with an anti-HA antibody. A3C-87 is A3C-28 with mutation L633 A, which disrupted the CLZ-mediated interaction without changing the charge of the construct. The position of A3C-87 indicates the monomer position of A3C-28. The two A3C-28 mutants, A3C-88 (K596E and R603E) and A3C-89 (D613K and E615K), had different mobilities in native-gel electrophoresis. When these two constructs are co-expressed, three bands are expected for a dimeric interaction (P_2, PQ and Q_2) and four bands for a trimer (P_3, P_2Q, PQ_2 and Q_3). Four bands were seen (indicated by arrowheads) when A3C-88 and A3C-89 were co-expressed. In the bottom panel, a fixed amount of A3C-88 was co-transfected with increasing amounts of A3C-89. Four bands can be clearly seen (arrowheads). **e**, Equilibrium analytical centrifugation. A 48-residue peptide corresponding to the CLZ domain (Lys 624 to Gly 671 of hCNGA3) was commercially synthesized and purified to more than 95% purity (Synpep, Dublin, CA). This peptide was acetylated at the N terminus and amidated at the C terminus, with a calculated M_r of 5,582. The peptide was subjected to analysis by equilibrium analytical centrifugation. A total of nine data sets were collected (0.5, 1.0 and 2.0 mg ml^{-1}, each spun at 40,000, 45,000 and 52,000 r.p.m.). A representative data set (2.0 mg ml^{-1} centrifuged at 40,000 r.p.m.; open grey squares) and its fitting curves are shown in the upper panel, with residuals (difference between data and fittings) in the lower panel. The data are best fitted by an ideal monomer–trimer model (red) with a M_r of 5,468 (confidence interval 5,375–5,559) and an association constant of 1.43×10^{10} M^{-2} (confidence interval (3.68–71.7) $\times 10^9$ M^{-2}). A similar fit with a monomer–dimer model gave an unrealistic M_r in excess of

7,000. With M_r fixed at 5,582 (the calculated value), neither the monomer–dimer (black) nor the monomer–tetramer models (green) fitted well.

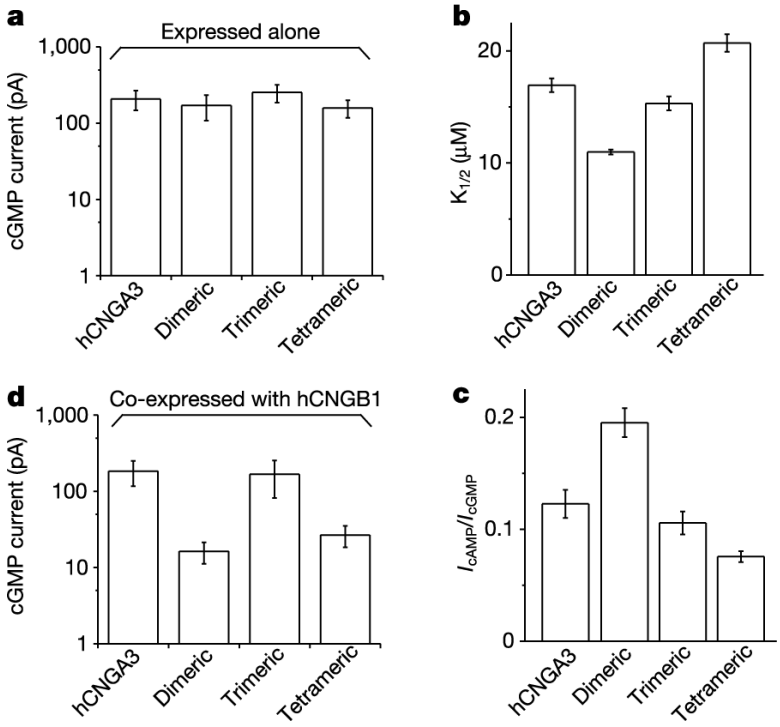

Figure 4.

Expression and functional properties of hCNGA3 and its CLZ-substituted mutants. Leu 626 to Val 669 of hCNGA3 was replaced, respectively, by well-characterized dimeric (LEDKVEELLSKNYHLENEVARLKKLVGERI), trimeric (IEDKIEEILSKQYHIENEIARIKKLIGERI) and tetrameric (IEDKLEEILSKLYHIENELARIKKLLGERI) leucine zippers. All transfections and subsequent recordings were performed side by side. **a**, Saturated cGMP-activated currents of homomeric channels formed by hCNGA3 and the three CLZ-substituted mutants, respectively. The values (means ± s.e.m.) are 207 ± 60 pA (hCNGA3, n = 12), 171 ± 63 pA (dimeric, n = 12), 253 ± 66 pA (trimeric, n = 12) and 159 ± 41 pA (tetrameric, n = 13). **b**, $K_{1/2}$ values of the cGMP dose–response relations for the wild-type and mutant channels. The values (means ± s.e.m.) are 16.9 ± 0.6 μM (hCNGA3, n = 8), 11.0 ± 0.2 μM (dimeric, n = 9), 15.3 ± 0.6 μM (trimeric, n = 9) and 20.7 ± 0.8 μM (tetrameric, n = 9). **c**, Saturated cAMP/cGMP current ratios of the wild-type and mutant channels. The values (means ± s.e.m.) are 0.122 ± 0.012 (hCNGA3, n = 9), 0.195 ± 0.013 (dimeric, n = 9), 0.106 ± 0.010 (trimeric, n = 9) and 0.076 ± 0.005 (tetrameric, n = 9). **d**, Saturated cGMP current produced by the co-expression of wild-type or mutant hCNGA3 with hCNGB1. The values (means ± s.e.m.) are 184 ± 67 pA (hCNGA3, n = 13), 16.3 ± 5.1 pA (dimeric, n = 14), 168 ± 86 pA (trimeric, n = 14) and 26.8 ± 8.4 pA (termeric, n = 14).

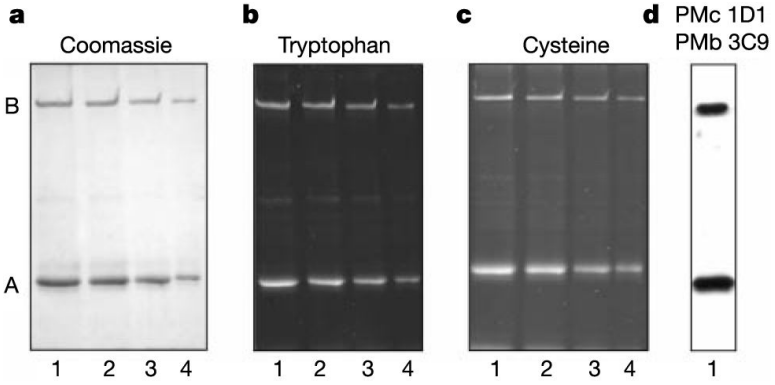

Figure 5.

Analysis of the A and B subunits of the native rod CNG channel. The CNG channel was purified from detergent-solubilized bovine rod outer segments on a PMc 1D1–Sepharose immunoaffinity column and analysed by SDS–PAGE and western blotting. **a**, Coomassie Blue-stained gel. **b**, Fluorescence from tryptophan residues modified by an ultraviolet-induced reaction of trichloroethanol and the channel. **c**, Fluorescence from Oregon Green maleimide-modified cysteine residues of the channel. **d**, Western blot labelled with a mixture of monoclonal antibodies, PMb 3C9 and PMc 1D1, against the B (M_r ~240K) and A subunits (M_r ~68K), respectively. Lanes 1–4 contained about 4, 3, 2 and 1 μg of protein, respectively.